Physical Model Simulations of Solar Thermal Energy Storage in Basaltic Rock Fills

Decho Phueakphum and Kittitep Fuenkajorn

School of Geotechnology, Institute of Engineering, Suranaree University of Technology,

Muang District, Nakhon Ratchasima, Thailand 30000.

Phone (66-44) 224-758, Fax (66-44) 224-448

E-Mail: d4740056@g.sut.ac.th

Abstract

The efficiency of solar thermal energy storage system using basaltic rock fills has been assessed using a scaled-down model. The proposed system is designed to operate without external electricity, as it is intended for poor people in remote and severely cold areas. During the daytime the solar energy is collected and stored in basalt ballasts filled in a shallow pit excavated above groundwater table. The surrounding soil and acrylic sheet cover serve as insulator. The stored thermal energy is released to warm up housing through a system of tubing at night. The thermal properties of ten rock types that are widely exposed in the north and northeast of Thailand are determined in the laboratory. A scaled-down model simulating the storage system and housing is constructed to monitor the temperature changes at various system components. Mathematical models are derived to compare with the monitoring results. Burirum basalt has been selected for testing as it poses the highest thermal conductivity and specific heat. The results indicate that throughout the night the system can increase the housing temperature by 4 to 6 Celsius higher than that of the surrounding, depending on the packing density, tube sizes and surrounding temperatures. The efficiency of this storage system is about 35 percents. The gained heat energy in the housing is equivalent to the electrical energy of 203.3 kJ·hr. The mathematical models developed here agree well with the measurement results.

1. Introduction

Local people in the north and northeast of Thailand have suffered from severely cold weather during winter. The temperature during winter in many areas drops to nearly zero Celsius [1]. Each year the government and public agencies have spent substantial funds (over 2.6 million US dollars for blankets and temporary shelters) to alleviate this problem [2]. The locals in these isolated areas are poor, and can not afford high-cost electrical energy. A long-term solution has called for a new low-cost technology that relies only on the renewable sources of energy and on locally available materials.

One of the feasible alternatives is the application of the solar thermal energy storage system. It deals with selecting the media that absorbs and stores heat during the daytime and releases it to warm housing space during the night. This technology is not new - it has long been studied and developed successfully in many countries with a variety of options for system components. Solar cells or solar greenhouse dome have sometimes been used to collect the thermal energy, and subsequently transferred by using a system of fan and tubing to the provided rock fills [3–7]. The advantage of this technology is that the sun is the main source of energy, which is not only enormous but also free. The rocks are relatively inexpensive, readily available in many areas, long-lasting and safe. Nevertheless, for the poor people the existing systems and their components are still expensive and difficult to install. The systems usually require external electricity to operate, and hence are not truly applicable for the remote areas.

RECEIVED 22 February, 2010

ACCEPTED 13 May, 2010

The objective of this research is to assess the performance of the solar thermal energy storage system in rock fills, without any support from the external electricity. The research effort involves determination of thermal properties of various rock types available in the north and northeast of Thailand, construction of a scaled-down model to demonstrate the system performance, derivation of mathematical governing equations to describe the temperature variation in the system, and development of a design guideline for a wide application of the proposed storage system in any specific areas.

2. Rock and Soil Properties

Ten rock types that are commonly found in the north and northeast of Thailand have been collected from the sites and tested in the laboratory to determine their mineral composition, specific heat and thermal conductivity. They can be categorized here into six groups: 1) four sandstones (Phu Kradung, Phu Phan, Phra Wihan, and Sao Khua sandstone), 2) three granites (Tak, Chinese, and Vietnamese granite), 3) two rock salts (Middle and Lower salt), 4) marble, 5) limestone, and 6) basalt. Soil sample was collected in the area of Suranaree University of Technology where the scaled-down model is constructed. From sieve analysis and hydrometer testing [8], the percentage by weight of gravel, sand, and clay are 17, 34 and 49 percent, respectively. Based on Unified Soil Classification System [9] the soil can be classified as clayey sand. Table 1 summarizes the thermal properties of the rocks and soil. The results indicated that Burirum basalt shows the highest specific heat (k_r) of 1,174 kJ/kg·K, and thermal conductivity (C_r) of 1.70 W/m·K, and hence has a good potential for thermal storage. It therefore has been primarily selected for rock fills in the scaled-down model. Figures 1 and 2 compare the thermal conductivity and specific heat of rocks tested here and from other research.

Table 1 Mineral compositions and thermal properties of rocks.

Rock Types	Density (g/cc)	Mineral Compositions	k_r (W/m·K)	C_r (MJ/m^3·K)
Compacted Soil	2.12	gravel 10-25%, sand 30-39%, Silt and Clay 47-51%	1.19 ± 0.00	2.43 ± 0.01
Saraburi Marble	2.58	calcite 100%	3.01 ± 0.00	2.91 ± 0.05
Burirum Basalt	2.81	pyroxene 50% and plagioclase 50%	1.70 ± 0.05	3.30 ± 0.71
Lopburi Limestone	2.64	calcite 100%	2.93 ± 0.00	2.54 ± 0.01
Phu Kradung Sandstone	2.54	lithic fragment 70%, quartz 18%, mica 7%, feldspar 3%, and other 2%	4.02 ± 0.01	1.80 ± 0.03
Phu Phan Sandstone	2.26	quartz 72%, feldspar 20%, rock fragment 3%, mica 3%, and other 2%	2.69 ± 0.01	2.00 ± 0.04
Phra Wihan Sandstone	2.33	quartz 75%, feldspar 15%, mica 7%, and lithic fragment 3%	3.75 ± 0.00	1.77 ± 0.02
Sao Khua Sandstone	2.33	feldspar 70%, quartz 18%, mica 7%, rock fragment 3%, and other 2%	2.06 ± 0.01	1.79 ± 0.02
Chinese Granite	2.64	plagioclase 70%, quartz 15%, orthoclase 7%, amphibole 5% and biotite 3%	3.16 ± 0.00	1.69 ± 0.01
Tak Granite	2.62	plagioclase 40%, quartz 30%, orthoclase 5%, amphibole 3% and biotite 2%	2.84 ± 0.00	2.21 ± 0.01
Vietnamese Granite	2.62	orthoclase 75%, quartz 10%, plagioclase 10% and amphibole 7%	3.26 ± 0.00	2.04 ± 0.03
Middle Salt	2.16	halite 98%, anhydrite 1%, clay mineral 1%	5.80 ± 0.01	1.83 ± 0.01
Lower Salt	2.19	halite 99%, clay mineral 1%	5.51 ± 0.01	2.54 ± 0.01

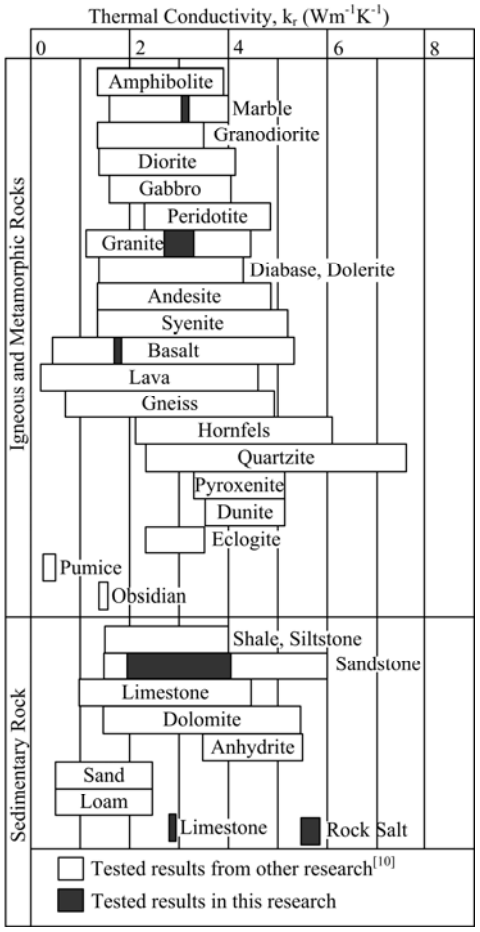

Figure 1 The thermal conductivity of rocks tested here and from other research compiled from Department Angewandte Geowissenschaften und Geophysik [10].

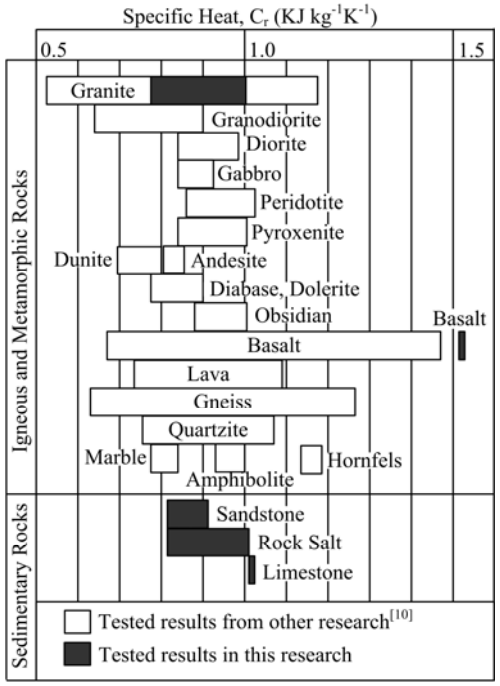

Figure 2 Heat capacity of rocks tested here and from other research compiled from Department Angewandte Geowissenschaften und Geophysik [10].

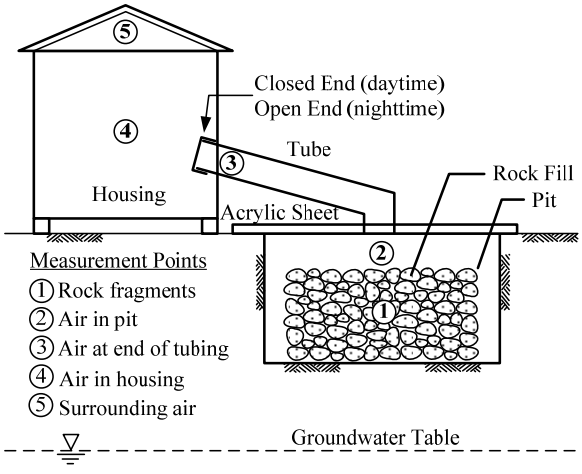

Figure 3 Conceptual of solar thermal energy storage in rock fills. The storage system (right) was connected to the housing model (left) by the hot-air tube. The hot-air tube was closed during charging period and was opened when using the collected energy.

3. Scaled-down Model

A scaled-down model was constructed to assess the efficiency of the solar thermal storage system and to determine its optimum design parameters. The system consists of two main components; a storage pit and a housing model (Figure 3). The storage medium (basaltic rock fills) absorbs the solar thermal energy and stores that energy in their mass causing an increase in temperature. The stored energy is released during nighttime to warm up the air in the housing model.

The storage pit (1.75×1.75×0.75 m^3) was filled with four chain-link baskets (0.5×0.5×0.5 m^3) packed with pre-defined fragment-sized basalt. Insulator sheets were placed around the pit walls and floor. The pit floor was excavated in soil mass above the groundwater table. Top of the pit was covered with a transparent acyclic sheet. The housing model was made of wood and covered with a tile roof. The insulator

sheets were applied around the pit walls and floor to prevent heat loss. The transparent acrylic sheets reinforced by steel frames were placed on top of the storage pit. This allows the solar energy to transmit to the rocks and to prevent the heat loss under mode of the force convection by wind. The housing model having a dimension of 1.5×1.5×1.5 m^3 was constructed with plywood. The housing model and the pit were connected via a hot-air tube. Several thermocouples were installed to monitor the changes of rock temperature at the center of pit, air in the pit, air at the end of the tube in the hosing model, air in the housing model, and the surrounding air (Figure 3). Figure 4 illustrate the scaled-down model for solar thermal energy storage.

3.1 Monitoring Results

The temperatures were monitored from the 20th of November 2005 through the 20th of April 2006, and from the 28th of November 2006 through the 21st January 2007. These represent the coldest periods during the year. The hot-air tubes with diameters of 5.1, 10.2 and 20.3 cm were used. To assess the effects of the amount of rock fill, the total weight of the rock fill of 743 kg was used and later changed to and 370 kg to assess the impact of the storage mass. Table 2 summarizes the test series set up for scaled-down model.

Figure 5a shows the temperatures as a function of time measured from the system with 5.1 cm diameter tubes with 743 kg rock fragments. Bottom end of the hot-air tube was placed on the top of the pit and the top end was inserted into the housing. The pit was not covered by any insulator on the top. During charging period (6:00 am-6:00 pm), the housing model was opened and the hot-air tube was shut. After 6:00 pm, the housing model was closed and the hot-air tube was opened to allow the hot-air in the pit to flow to the housing model and the cool-air in housing model circulated back to the pit. Results from the temperature measurements indicated that the heat flow through the pipe to the housing space was minimal, probably due to excessive heat loss through the acrylic sheet, improper size of the tube, and leakage of heat energy of the housing model.

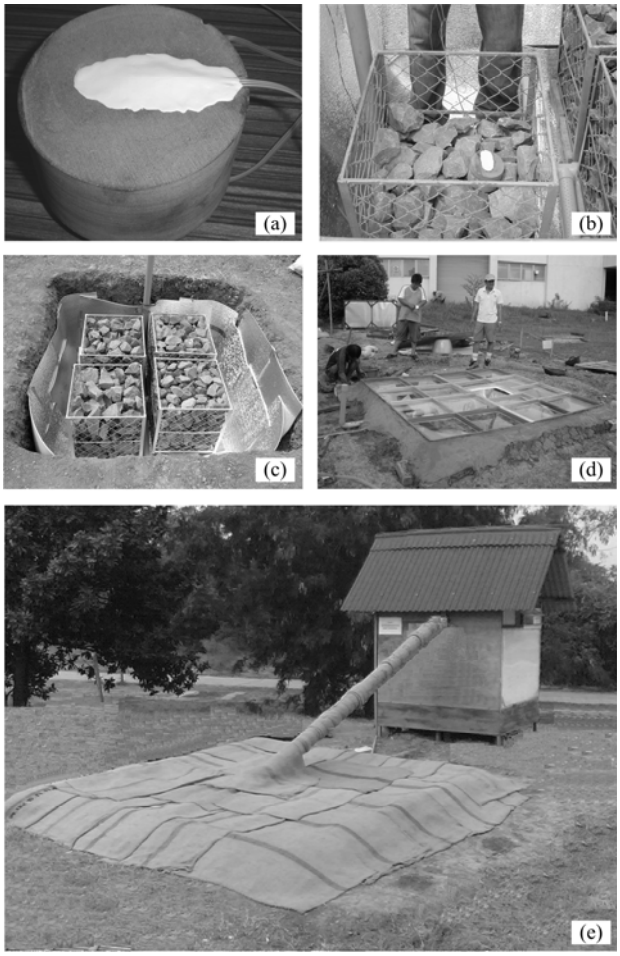

Figure 4 Scaled-down model for solar thermal energy storage. (a) thermocouple attached in surface of rock fragment, (b) rock fragment with thermocouple is laid in rock basket, (c) baskets of rock fragment, (d) Acrylic sheet reinforced with steel frame, and (e) storage system connected to housing with tube.

In an attempt to enhance the heat flow, the hot-air tube with a diameter of 10.2 cm was installed. It was inclined at an angle of 30 degrees. The tube was covered with an isolator prevent the heat loss by conduction to the surrounding. The opening and closing times for the pit, tubes, and housing was same as the previous testing. The

Table 2 Series of monitored results from scaled-down model.

Test series	Monitoring Duration	Rock Weight	Tubing Diameter and Inclination	Remarks
I	Nov 20, 2005 – Dec 14, 2005	743 kg	5.1 cm 0°	Don't cover on top of pit OH, OP and CT – 6:00 am/CP, CH and OT – 6:00 pm
II	Dec 18, 2005 – Jan 4, 2006	743 kg	10.2 cm 30°	Covered on the top of pit OH, OP and CT – 6:00 am/CP – 3:00 pm; CH and OT – 9:00 pm
III	Jan 6, 2006 – Apr 20, 2006	743 kg	20.3 cm 60° (first half) 20° (second half)	Covered on the top of pit OH, OP and CT – 9:00 am/CP – 3:00 pm; CH and OT – 9:00 pm
IV	Nov 28, 2006 – Jan 21, 2007	370 kg	20.3 cm 60°/ 20°	Covered on the top of pit OH, OP and CT – 9:00 am/CP – 3:00 pm; CH and OT – 9:00 pm

O = Open; C = Close; P = Pit (Rock fills); T = Hot-air tube; H = Housing

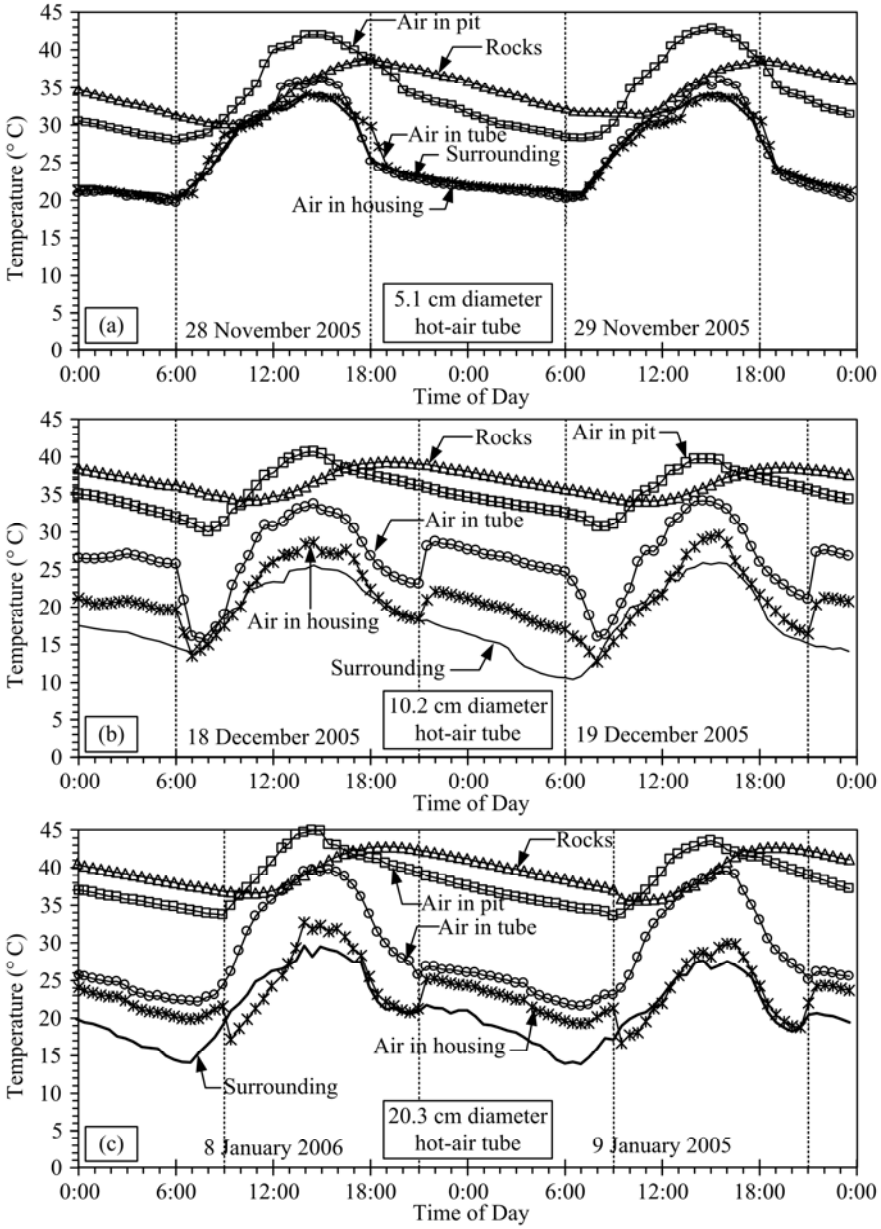

Figure 5 Temperature as a function of time measured from various components using the hot-air tube with diameter of 5.1-cm (a), 10.2 cm (b), and 20.3 (c).

housing model was opened and the tubes were closed after 6:00 am. After 9:00 pm the housing was closed and the tubes were opened. The measurement results were not different from the previous test. This is probably because there were significant energy losses on the top of the pit.

To prevent the energy loss, the top of the pit was covered by gunny-bags after 3:00 pm. The temperature in housing model was increased by about 1 Celsius higher than that of the surrounding. Then the housing walls, ceiling and floor were sealed with 2-cm thick polyurethane foam sheets to minimize the heat loss and leakage. After the tubes were opened, the temperature in the housing model rapidly increased within the first 60 minutes then its slightly decreased which was similar to the increasing rate of air in the hot-air and surroundings. The result showed that more heat energy was transferred to the housing model as evidenced by the temperature in the housing model was nearly 5 Celsius higher than the surrounding temperature (Figure 5b).

Figure 5c shows the temperature as a function of time measured from the system using 20.3 cm diameter hot-air tube with 743 kg of rock fragments. The tube was inclined at an angle of 60 degrees on the first half and 20 degrees on the second half. The elevation difference between the inlet and outlet was about 1.5 m. The opening and closing times of the pit, housing model, and tubes were the same as the previous. The temperature changes were similar to the results obtained from the system with 10.3-cm diameter hot-air tube. The results indicated that the temperature increasing in the housing model was greater than 5 Celsius.

To study the effect of rock fragments quantity, the system with 20.3-cm diameter hot-air tube is took about 50% of the rock fragment out off (the remaining weight was approximately 370 kg). The housing model was opened at 9:00 am and the storage pit was also opened at 9:00 am. After 3:00 pm, the pit was closed again and the hot-air tube was opened at 9:00 pm. The measured temperature in the housing model increased around 2-3 Celsius (Figure 6) over the surrounding temperature which was about 50% of the temperature increasing compared to the previous model where the rock fragments was not removed.

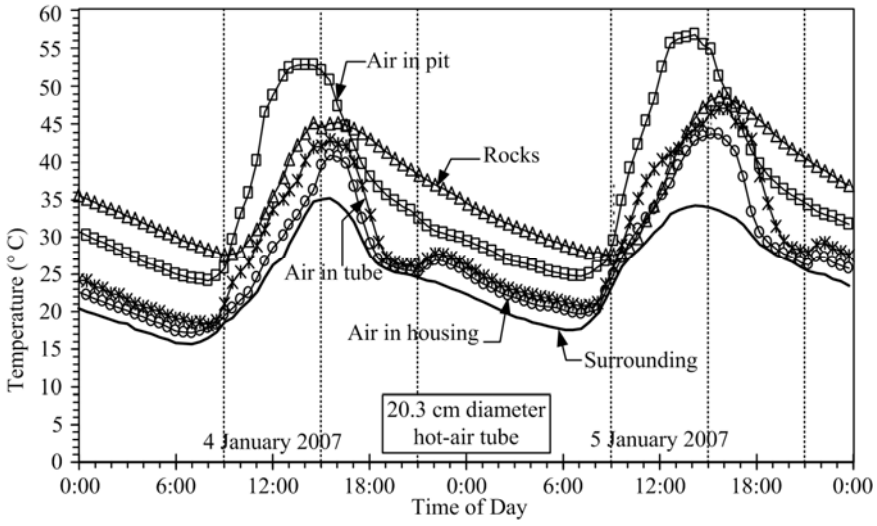

Figure 6 Temperature as a function of time various components using 20.3-cm diameter hot-air tube and 370-kg rock fragment.

3.2 Discussion of results

The results suggest that storage system efficiency depends on the level of energy input, size and inclination of hot-air tube, heat losses from the pit and housing. It seems that the most suitable model is the system at which the storage pit is connected to the housing model using 10.2-cm (4 inches) diameter hot-air tube and inclined at about 30 degrees. The top of storage pit should be covered with the isolator sheet (a textile, gunny-bags or fabric sheet). This arrangement provides a temperature increase up to 5 Celsius in the housing model. When the heat energy was allowed to transfer to the housing model until 9:00 am, the temperature in the storage pit is still higher than that in the housing model. This implies that the efficiency of the heat transfer was not optimized. Mathematical model is therefore needed to improve efficiency of the system (to be discussed in the next section).

4. Development of Mathematical Models

A mathematical model was developed from the energy balance equations to determine the thermal variations in each component of the scaled-down model. Figure 7 shows the parameters and variables used in the derivation. The system comprises three controlled volume system; 1) rock fragments (CV_1), air in storage pit (CV_2), and air in housing model (CV_3).

The mathematical calculations are carried out under the principle of energy balance. Each system is presented with various modes of heat transfer; radiation, convection, and conduction, which result in a very complicated and difficult problem. To minimize the complications and difficulty, the following assumptions are posed: (i) the solar energy (I_s) is absorbed by the air is neglected, (ii) the humidity in the air is neglected, (iii) the physical parameters are assumed to be constant, (iv) the thermal gradient within solid particles is neglected, (v) radiation effects are neglected, (vi) radial heat transfer does not occur, (vii) losses to the environment are ignored, (viii) internal heat generation is absent and heat flow is one dimensional and in quasi-steady state condition. An energy balance is performed on the fluid (air in pit) and solid (rock fragments) phases, yielding a coupled set of partial differential equations for each component.

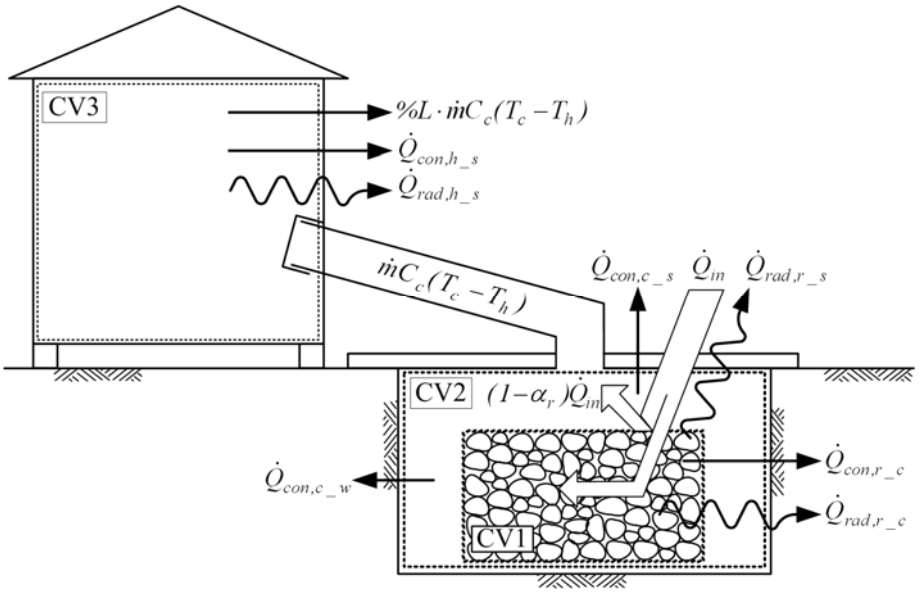

Figure 7 Heat transfer modes within rock fill (CV1), pit air (CV2) and housing (CV3).

4.1 Daytime equivalent model

The solar radiation (I_s) transmitted through the transparent acrylic sheet is absorbed by the rock fill. The ability of rocks to store the energy depends on the thermal absorbability (α_r). The temperature of the rock bed increases and the heat is then transferred to the flowing air by convection, and to the pit walls and floor by convection and radiation. The air is heated up along its path and loses some of heat transfer mechanisms through various heat transfer coefficients (Figure 7).

The rock fill system (CV_1) is a close system. The energy gained in mass of rock is from the rock fill absorbed the incident solar radiation ($\dot{Q}_{in}$). There are three sources of heat loss from the rock fill; 1) radiative heat transfer ($\dot{Q}_{rad,r\_c}$) from rock fill to the pit air, 2) radiative heat transfer ($\dot{Q}_{rad,r\_s}$) from rock fill across the acrylic sheet to the surrounding air, and 3) convective heat transfer ($\dot{Q}_{con,r\_c}$) from rock fill to pit air. The governing equation can be expressed in the form of transient state or unsteady state as:

$$\frac{E_{CV1}}{dt} = \dot{Q}_{in} - \dot{Q}_{rad,r\_c} - \dot{Q}_{rad,r\_s} - \dot{Q}_{con,r\_c} \tag{1}$$

It is assumed that the temperature of pit wall is the same as that of the air in the pit.

$$m_r C_r \frac{dT_r}{dt} = \alpha_r I_s A_{r,top} - \sigma\varepsilon_r A_{rad}(T_r^4 - T_c^4) - \sigma\varepsilon_r A_{r,top}(T_r^4 - T_s^4) - h_r A_r (T_r - T_c) \tag{2}$$

where m_r = the mass of rocks in pit (kg),

C_r = the specific heat or heat capacity of rocks (J/kg·K),

α_r = absorptivity coefficient of rocks,

I_s = solar radiation or heat flux (W/m^2),

$A_{r,top}$ = solar collection area which equivalent to the area of rocks on the top exposed to the air (m^2),

σ = the Stefan-Boltzmann constant (= 5.67×10^{-8} W/m^2·K^4),

ε_r = emissivity or heat exchanger effectiveness of the rock,

A_{rad} = the surface of emissivity (m^2),

T_r = the rock temperature (K),

T_c = the pit air temperature (K),

T_s = the surrounding temperature or air outside the housing (K),

h_r = convective heat transfer coefficient from rocks to air (W/m^2·K) and

A_{rad} = the area of all rock fragments (m^2).

The Euler's method [11–12] is applied to obtain the solution. Eq. (2) becomes

$$m_r C_r \frac{T_r^n - T_r}{\Delta T} = \alpha_r I_s A_{r,top} - \sigma\varepsilon_r A_{rad}(T_r^4 - T_c^4) - \sigma\varepsilon_r A_{r,top}(T_r^4 - T_s^4) - h_r A_r (T_r - T_c) \tag{3}$$

Here, T_r^n is the temperature of the rock at the next time step. Δt is the time interval between each step. Rearranging Eq. (3) we obtain;

$$T_r^n = T_r + \frac{\Delta t}{m_r C_r}\left[\alpha_r I_s A_{r,top} - \sigma\varepsilon_r A_{rad}(T_r^4 - T_c^4) - \sigma\varepsilon_r A_{r,top}(T_r^4 - T_s^4) - h_r A_r (T_r - T_c) \right] \tag{4}$$

For the calculations in the following time step, T_r is taken as T_r^n, and the calculations continued till the required final time.

Assuming that the mode of heat transfer from the rocks to the surrounding air is by natural convection, and the rock fragments are spherical shape, the convective heat transfer coefficient (h_r) is a function of Nusselt number (Nu),

characteristic length (δ) and thermal conductivity coefficient (k) of the rocks:

$$h_r = \left(\frac{k}{\delta}\right)Nu \tag{5}$$

For spherical shape with diameter D, δ is equal to ½ πD, and Nu is dependent of the characteristics of surface

$$Nu = 2 + \frac{0.589Ra^{1/4}}{\left[\left[1+\left(\frac{0.469}{Pr}\right)\right]^{9/16}\right]^{4/9}} \tag{6}$$

where Pr is Prandtl number of dry air under atmospheric pressure which equal to 0.71 under temperature 0 through 300 Celsius and Ra is Rayleigh number ($\leq 10^{11}$ when $Pr \geq 0.7$) [13].

Air in the storage system (CV_2) gains its energy by the solar heat emitted from the rock fill ($(1-\alpha_r)\dot{Q}_{in}$), radiative and convective heat transfers from rock fill. It loses energy by heat convection to the surrounding air above the acrylic sheet ($\dot{Q}_{con,c\_s}$) and to the pit wall ($\dot{Q}_{con,c\_w}$):

$$\frac{dE_{CV2}}{dt} = (1-\alpha_r)\dot{Q}_{in} + \dot{Q}_{rad,r\_c} + \dot{Q}_{con,r\_c} - \dot{Q}_{con,c\_s} - \dot{Q}_{con,c\_w} \tag{7}$$

$$T_c^n = T_c + \frac{\Delta t}{m_c C_a}\left[f_{ab}(1-\alpha_r)I_s A_{r,top} + \sigma\varepsilon_r A_{rad}(T_r^4 - T_c^4) + h_r A_r(T_r - T_c) - U_1 A_{acr}(T_c - T_s) - U_2 A_w(T_c - T_{soil})\right] \tag{8}$$

where m_c = the mass of air in storage system (kg),

C_a = the specific heat of the air (J/kg·K), ranging from 1,012 J/kg·K through 1,017 J/kg·K,

f_{ab} = the heat loss factor from reflected radiation of rock,

A_{acr} = the area of acrylic sheet (m^2),

A_w = the area of the pit wall (m^2),

U_1 = overall heat transfer coefficient of air from pit to surrounding air ($W/m^2 \cdot K$),

U_2 = overall heat transfer coefficient of the air to the pit wall ($W/m^2 \cdot K$).

$$U_1 = \frac{1}{\frac{1}{h_{ic}} + \frac{\Delta x}{k_{acr}} + \frac{1}{h_{exc}}} \text{ and } U_2 = \frac{1}{\frac{1}{h_i} + \frac{\Delta x}{k_{acr}}} \tag{9}$$

where Δx = the thickness of acrylic sheet (m),

h_{ic} = convective heat transfer coefficient of air in pit ($W/m^2 \cdot K$),

h_{exc} = convective heat transfer coefficient of air outside the pit or air above cover sheet ($W/m^2 \cdot K$),

k_{acr} = thermal conductivity of acrylic sheet ($W/m^2 \cdot K$).

The value of h_{ic} and h_{exc} can be evaluated by using Eq. (5).

The mass of air (m_c) in storage system can be calculated from the cross product between the density of air (ρ_{air}) and the volume of pit (V_c). The density of air is a function of temperature; it decreases when the temperature increases. The density of air is 1.197 kg/m^3 at temperature of 22 Celsius and decreases to 1.054 kg/m^3 at temperature of 62 Celsius. For simplicity the air density is assumed to be constant at 1.103 kg/m^3.

4.2 Nighttime equivalent models

The systems during nighttime when the stored energy is used are divided into three subsystems, including rocks in the pit (CV_1), air in the pit (CV_2) and air in the housing model (CV_3). When the lid of the hot tube is opened, the hot air immediately flows through the tube to the housing model. The heat transfer during the nighttime is similar to that during daytime, but without the external energy source (solar energy). The heat loss from solar radiation in the rocks to the

surroundings is nil due to the acrylic sheet and the isolated cover. The energy equations of rocks and air in storage system, Eqs. (4) and (8), can then be re-written as:

$$T_r^n = T_r + \frac{\Delta t}{m_r C_r}\left[\begin{array}{l} -\sigma\varepsilon_r A_{rad}(T_r^4 - T_c^4) \\ -h_r A_r\left(T_r - T_c\right) \end{array}\right] \quad (10)$$

$$\begin{aligned} T_c^n = T_c + \frac{\Delta t}{m_c C_c}\Big[&\sigma\varepsilon_r A_{rad}(T_r^4 - T_c^4) + h_r A_r (T_r - T_c) \\ &- U_1 A_{acr}(T_c - T_{sur}) - U_2 A_{cham}(T_c - T_{soil}) \\ &- \dot{m} C_a (T_c - T_h)\Big] \end{aligned} \quad (11)$$

where $\dot{m}$ is an air mass flow rate from the storage pit to the housing (kg/s) under stack effect when the hotter air (in pit) flows to the cooler area (in housing). Bansal et al [14] and Anderson [15] propose the equation to determine the air mass flow rate as follows:

$$\dot{m} = \frac{(P/R\cdot T_c)\rho_c C_D A_o}{\sqrt{1+(A_o/A_i)}}\sqrt{2gH\left(\frac{T_c - T_h}{T_c}\right)} \quad (12)$$

where P = air pressure (= 101,300 Pa),

C_D = discharge coefficient (= 0.60 through 0.75),

R = gas constant (= 287 J/ Kg·K),

C_a = specific heat of air (kJ/kg·K),

T_h = temperature of air in housing (K),

A_o = the outer cross-sectional areas of tube (m^2),

A_i = the inner cross-sectional areas of tube (m^2),

A_r = ratio of A_o/A_i, and

H = elevation head of tube (different between the elevation of entrance and exit (m).

The mass of hot air in storage system ($\dot{m}C_a(T_c - T_h)$) flows to the housing space and causing an increase in the temperature of in the housing. At the same time, there is heat loss to the surroundings by convection ($\dot{Q}_{con,h\_s}$) and radiation ($\dot{Q}_{rad,h\_s}$), and leaks ($\dot{Q}_{leak}$) of air in housing through the gaps. The energy leaks (%L) are assumed to be 0 to 15% of energy from air mass flow from the storage system. The energy equations of air in housing are shown below:

$$\frac{dE_{CV3}}{dt} = \dot{m}C_a(T_c - T_h) - \dot{Q}_{con,h\_s} - \dot{Q}_{rad,h\_s} - \dot{Q}_{leak} \quad (13)$$

$$\begin{aligned} T_h^n = T_h + \frac{\Delta t}{m_h C_a}&[(1-\%L)\cdot\dot{m}C_a(T_c - T_h)] \\ &- U_h A_h (T_h - T_s) - \sigma\varepsilon_h A_h (T_h^4 - T_s^4) \end{aligned} \quad (14)$$

where U_h = overall heat transfer coefficient of air in housing to surroundings ($W/m^2\cdot K$),

m_h = mass of air in the housing (kg),

$h_{i,h}$ = convective heat transfer coefficient of air in the housing ($W/m^2\cdot K$),

$h_{ex,h}$ = convective heat transfer coefficient of air outside housing ($W/m^2\cdot K$),

k_w = thermal conductivity coefficient of housing wall ($W/m\cdot K$),

A_h = area of housing wall for thermal loss (m^2),

Δx = thickness of housing wall (m).

The values of $h_{i,h}$ and $h_{ex,h}$ can be determined from Eq. (5).

5. Comparisons of the Results

This section compares the temperatures measured from the scaled-down model with those calculated from the mathematical model. The objective is to assess the reliability, the agreement, and the variability of the results. The input parameters for the calculation include the constants and variables related to the characteristics of the storage pit, hot-air tube, and housing model. The constant parameters include the surrounding air obtained from the recorded of Thai Meteorological Department [1], the soil mass temperature obtained from the measured results, the solar

radiation calculated from the equation proposed by Exell and Kumar [16], the air properties; density, Nusselt number, Prandtl number, specific heat and thermal conductivity [17], the rock properties (a specific heat and thermal conductivity, emissivity, absorbtion coefficient, effective diameter), and the acrylic sheet properties (a specific heat and thermal conductivity, thickness, area). Table 3 summarizes the solar radiation, temperature of soil mass and temperature of surrounding air as a function of time using in the calculation. Table 4 summarizes the constant parameters of rock and acrylic sheet used in the calculation.

Table 3 Input data for the calculation: solar radiation, temperature of soil mass and surrounding air.

Time of Day	Solar Radiation* (W/m^2)		Temperature (°C)		
			Surrounding Air**		Soil Mass***
	Avg.	Min	Avg.	Min	
06:00	58.4	19.5	19.2	10.4	28.5
07:00	185.2	133.7	20.2	10.7	28.4
08:00	323.8	258.4	22.4	12.8	28.8
09:00	457.3	364.9	24.6	15.9	29.3
10:00	567.0	450.8	26.8	18.8	29.8
11:00	636.2	496.0	28.9	21.3	30.3
12:00	653.8	493.8	31.0	23.9	30.8
13:00	617.2	446.2	32.7	25.9	31.3
14:00	532.1	361.9	33.7	26.9	31.9
15:00	411.9	256.5	33.9	27.3	32.3
16:00	274.5	147.8	32.3	26.8	32.4
17:00	138.3	51.8	29.4	25.1	32.2
18:00	21.2	0	26.0	22.5	31.9
19:00	0	0	23.5	20.2	31.7
20:00	0	0	22.4	18.5	31.4
21:00	0	0	22.0	17.0	31.1
22:00	0	0	21.6	15.6	30.8
23:00	0	0	21.3	14.6	30.5
24:00	0	0	20.9	14.0	30.2
01:00	0	0	20.6	13.4	29.9
02:00	0	0	20.1	12.8	29.6
03:00	0	0	19.7	12.2	29.4
04:00	0	0	19.4	11.6	29.1
05:00	0	0	19.0	11.3	28.8

* Using equation proposed by Exell and Kumar[15]

** Records by Thai Meteorological Department[1]

*** Measure from scaled-down model

The variables include the characteristics of the storage pit (width, length, and depth), packed rock fragment properties (weight, collector surface and thickness), characteristics of the hot-air tube (diameter, inclination, length and elevation head between inlet and outlet), and the volume of housing model. An unknown for this study is the percentage of heat energy leaking from the housing model. This unknown is determined from the measurement results. The computer program, MATLAB version 7.0, is used in the calculation. Euler's method for the integration of mathematical equation is applied.

Fig. 8(a) through Fig. 8(c) compares the changes of air temperature in the housing model and the surrounding air using 5.1, 10.2, and 20.3 cm diameter hot-air tube with 743 kg of rock fragments. Fig. 8(d) compares the results using 20.3 cm diameter hot-air tube with 370 kg of rock fragments. The results from the two methods are similar. The larger hot-air tube provides a higher temperature at the housing model. The housing temperature is about 3–6 Celsius higher than that of the surrounding air. The calculation results suggest that about 10 percent of heat energy is leaked from the housing model. The calculated results agree well with the measurement results which can be concluded that the derived mathematical equations are reliable and suitable for the temperature predictions under different parameters.

Table 4 Constant parameters of rock and acrylic sheet used in the calculation.

Parameters	Unit	Value
a) Rock fragment		
- Specific heat, C_r	J/kg·K	1,174
- Thermal conductivity, k_r	W/m·K	1.70
- Effective diameter, D_{eff}	m	0.08
- Emissivity, ε_r	-	0.8
- Absorbtion coefficient, α_r	-	0.8
- Density, ρ_r	kg/m^3	2,760
b) Acrylic sheet		
- Specific heat, C_a	J/kg·K	1,470
- Thermal conductivity, k_a	W/m·K	0.20
- Thickness, t_a	m	0.003
- Density, ρ_a	kg/m^3	1,150

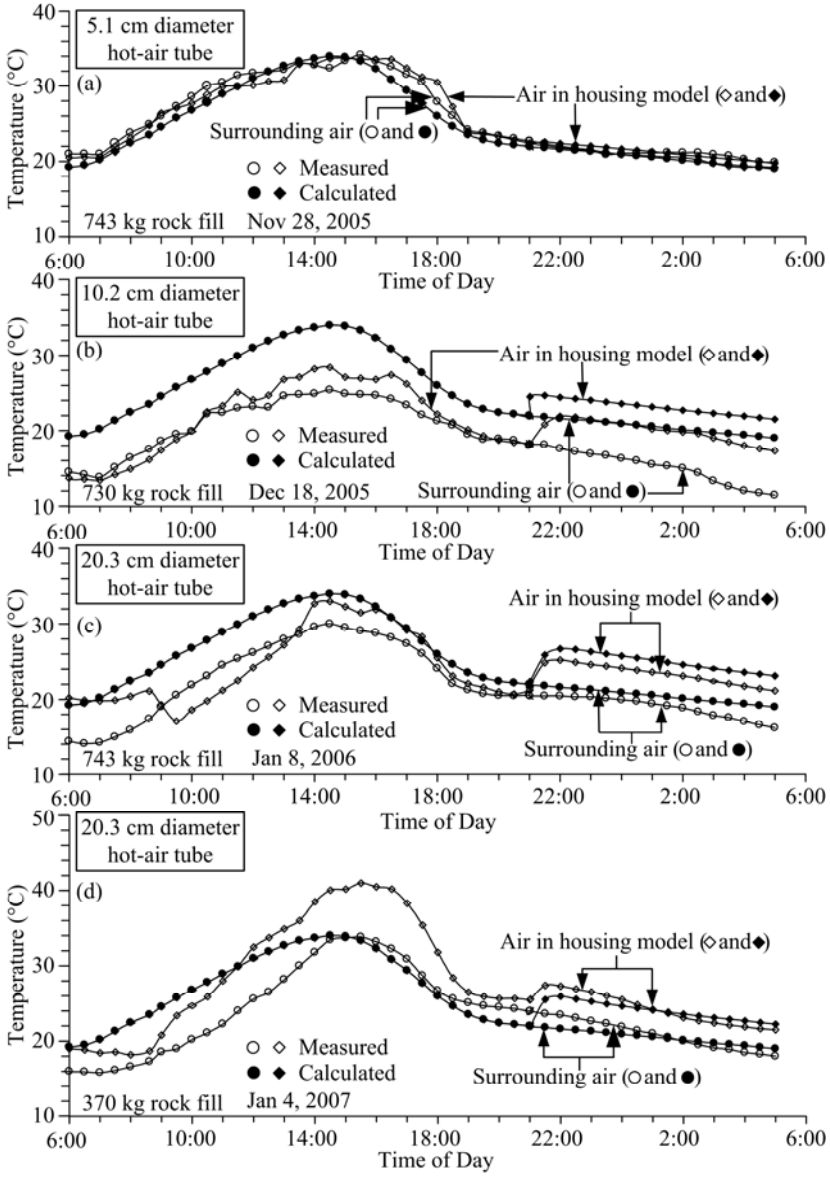

Figure 5 Comparisons of temperature variation of the air in housing model (square dots) and the surrounding air (circle dots) from scaled-down model (light dots) with those the calculated results using mathematical equation (solid dots).

6. Performance of Storage System

An attempt is made here to assess the storage system efficiency and to determine the heat energy gained in the housing in form of electrical energy. The housing model with 10.2 cm diameter hot-air tube is considered here as an example. The amount of solar energy stored (Q_r) in the rock fill due to the direct gain of solar energy, with the mass flow rate of air being zero, is given by:

$$Q_r = m_r C_r \Delta T = [V_{bed} (1 - \varepsilon) \rho_r] C_r \Delta T \qquad (15)$$

where ΔT = the rock fragments temperature increase over a specified period of time,

C_r = the specific heat of the rocks,

m_r = the weight of the rock fragment,

V_{bed} = the bulk volume of rock or the packed rock volume;

ε = the void fraction of rock fill (= 0.50), and

ρ_r = the density of rocks (= 2,760 kg/m^3).

The storage efficiency (η) of the rock fill is given by:

$$\eta = Q_r/I \quad (16)$$

where I is the amount of solar radiation received over a specified period of time [18].

From the observations in the scale-down model, the average temperature increase of rock fragments is about 5 Celsius. The solar energy stored in the rock fill is estimated as 4.28 MJ. The amount of solar radiation received over a specified period of time (during 9.00 am – 3.00 pm) is estimated as 12.4 MJ. The efficiency of this storage system is about 35%. By using the absorbed energy equation proposed by Sonntag et al [19], the gained heat energy in housing is equivalent to the electrical energy of 203.3 kJ·hr.

7. Discussions and Conclusions

The mathematical equations are used to improve the system efficiency by producing comparable temperatures in the housing and storage pit, during the heat transfer time. The heat transfer is simulated to compare with the actual temperature measured in the model. The calculated results agree with the measurements which can be concluded that the mathematical equations are reliable and suitable for the temperature predictions under different physical parameters. The heat loss from the housing model is calibrated at 10 percent of the total heat energy transfer. The variables from the sensitivity analysis including volume of the housing model, packed rock volume, collector area, and size of the hot-air tubes are considered for the design recommendations.

From the observations on the scaled-down model it seems that the soil mass around the pit was not completely dry. The permeated water would be evaporated and suspended in the hot air mass and then transferred to the housing model. When the air in the housing cooled down in the morning, the vapor is condensed to be the drop of water on the ceiling. To solve this problem, the pit walls and floor should be covered with the impermeable material such as concrete, steel sheet, or rubber. This can increase the efficiency of rock fragments to store the heat energy due to the heat loss to soil mass was minimized. The efficiency of the storage pit and the increasable of housing temperature can be improved by several ways such as installation of ventilator at the hot-air tube increases the mass flow rate from the storage and temperature in the housing model, installed double layers of acrylic sheet on the top of pit, cover the pit walls and floor with impermeable material with also can prevent the heat loss. Some housing with the wall made from bamboo should be covered with the isolator.

8. Acknowledgement

This research is funded by Suranaree University of Technology. Permission to publish this paper is gratefully acknowledged.

References

[1] Thai Meteorological Department (2003) Climate Information Service (in CD-ROM).

[2] Department of Disaster Prevention and Mitigation (2005). Summary of disaster situation in the winter season during 2000 through 2005 [On-line]. Available: http://www.disaster.go.th/disaster01/disas_05.xls.

[3] Coutier JP, Farber EA (1982) Two applications of a numerical approach of heat transfer process within rock beds. Sol. Energy 29, 451-462.

[4] Meier A, Winkler C, Wuillemin S (1991) Experiment for modeling high temperature rock bed storage. Sol. Energy 24, 255-264.

[5] Choudhury C, Chauhan PM, Garg HP (1995) Economic design of a rock bed storage device for storing solar thermal energy. Sol. Energy 55, 29-37.

[6] Abbud IA, Löf GOG, Hittle DC (1995) Simulation of solar air heating at constant temperature. Sol. Energy 54, 75–83.

[7] Kurklu A, Bilgin S, Ozkan B (2003) A study on the solar energy storing rock-bed to heat a polyethylene tunnel type greenhouse. Renewable Energy 28, 683-697.

[8] ASTM D422–63. Standard Test Method for Particle-Size Analysis of Soils. AS Annual Book of ASTM Standards, Vol. 04.08. West Conshohocken, PA: ASTM.

[9] ASTM D2487–06e1. Standard Practice for Classification of Soils for Engineering Purposes (Unified Soil Classification System). Annual Book of ASTM Standards, Vol. 04.08. West Conshohocken, PA: ASTM.

[10] Department Angewandte Geowissenschaften und Geophysik. (2006). Chapter 8: Thermal Properties of Rocks [On-line]. Available: http://www.unileoben.ac.at/ ~geophwww/ neu/data/chapter8thermal.pdf

[11] Chapra SC (2005) Applied numerical methods with MATLAB for engineers and scientists. McGraw-Hill, Boston.

[12] Chapra SC, Canale RP (2002) Numerical Methods for Engineers. McGraw-Hill, New York.

[13] Raznjevic K (1976) Handbook of thermodynamics tables and charts. McGraw-Hill, New York.

[14] Bansal NK, Mathur R, Bhandari MS (1993) Solar chimney for enhanced stack ventilation. Build. Environ. 28, 373–377.

[15] Anderson KT (1995) Theoretical considerations on natural ventilation by thermal buayance. Transaction of American Society of Heating, Refrigerating and Airconditioning Engineers 101, 1103–117.

[16] Exell RHB, Kumar R (1981) Solar radiation tables for architects in Thailand. AIT research no. 128, Asian Institute of Technology, Bangkok, Thailand.

[17] Cengel YA (1997) Introduction to thermodynamics and heat transfer. Springer-Verlag, New York.

[18] Hamdan MA (1998) Investigation of an inexpensive solar collector storage system. Energy Convers. Manage. 39, 415-420.

[19] Sonntage RE, Borgnakke C, VanWylen GJ (1998) Fundamentals of Thermodynamics. 5th edn, John Wiley & Son, New York.